Article

Gradient Heatmetry in a Burners Adjustment

Pavel G. Bobylev * , **Andrey V. Pavlov, Vyacheslav M. Proskurin, Yuriy V. Andreyev, Vladimir Yu. Mityakov and Sergey Z. Sapozhnikov**

Science Educational Center "Energy Thermophysics", Peter the Great St. Petersburg Polytechnic University (SPbPU), St. Petersburg 195251, Russia
* Correspondence: bobylev_pg@spbstu.ru; Tel.: +7-812-552-7773

Abstract: Measuring the heat flux in the furnace of industrial boilers is an urgent task in the power industry. Installing the measuring instruments directly into the furnace is a laborious and complex process. It requires a complete shutdown of the boiler, which incurs economic costs. It is most efficient to use portable probes with measuring insert. The created cooled probe with a heterogeneous gradient heat flux sensor is a unique and versatile tool that allows for the configuration and control of the operation of power boilers. This article compares experimental values with calculation methods. The obtained heat flux per unit area is in good agreement with the theoretical concepts when the values are averaged. The technique used in this paper makese it possible to determine the maximum heat-stressed zones and areas with stable or unstable combustion. The main combustion zones that are typical for the flaring of any fuel are identified. This approach allows us to consider various approaches to heat transfer enhancement during the combustion of both liquid and gaseous fuels. Comparison of experimental results with the data of other authors is not quite exact due to the complexity of the experiment. The study of burners in this configuration has not previously been considered in the literature.

Keywords: gradient heatmetry; gradient heat flux sensor; burner; gas combustion; diesel combustion

1. Introduction

Uneven heat generation and flame instability depend on many factors, for example, the guiding device, oxidant supply system, fuel supply system malfunctions, etc. Power equipment time lag leads to difficulty in identifying problems with the burner as they arise. Generally, two sensors control the operation of the burner: the flame sensor and the fuel flow rate meter. Their data make it possible to analyse burner malfunctions only in cases of emergency, and it is impossible to detect the origin of malfunction.

Differences in boiler equipment design features makes monitoring more complicated. In fire-tube boilers, irregularity of heat generation, unstable flame, etc., can cause burnout of the fire tube, which is fatal for the entire power plant. Usually, boilers of this type are low-power and have one burner, which makes them easier to control. In high-power water-tube boilers with several burners, it is impossible to monitor the malfunction of each burner.

Currently, there is no methodology for calculating local heat generation from the flame. All functional connections have the form [1,2]:

$$Q = f(\dot{M}, Q_{LHV}) \tag{1}$$

where Q (W, watts) is the heat generated by fuel combustion, $\dot{M}$ (kg/s) is the fuel mass flow rate, and Q_{LHV} (J/kg) is the fuel lower heating value.

The dependence on (1) makes it possible to estimate the average heat generation during fuel combustion only, not the distribution of the flame local heat flux. Most experiments and practical monitoring of thermal equipment have been conducted using temperature

measurement. In spite of the need to measure the heat flux per unit area and not the temperature, there are significantly fewer primary converters for measuring heat flux than invasive and non-invasive thermal sensors.

The most interesting and valuable paper in this regard is the investigation by D. Zhang et al. [3], where a probe for measuring the heat flux from a flame was presented. As stated above, its principle of operation is based on temperature measurement. The measuring insert has the form of a solid cylinder with two thermocouples mounted on the cylinder axis. For this design, the probe sensitivity is determined by the temperature difference. With an increase in the distance between the thermocouples, the sensitivity increases, while the response time decreases. In accordance with the obtained data, the authors identified an optimal distance for the experimental conditions of 8 mm. This probe made it possible to consider the heat generated from the torch in the furnace of a 600 MW supercritical arch-fired boiler (SC-AFB). Measurement of the heat flux in aggressive media can be performed using sensors which are a set of thermocouples [3].

Another common way to measure heat flux from a flame is to use a diffusion-type Gardon Gauge. Its application in combustion is good, as shown in [4]. The design of the sensor is shown in Figure 1. It consists of a thin piece of circular constantan foil attached to a massive copper radiator, which is the sensor housing.
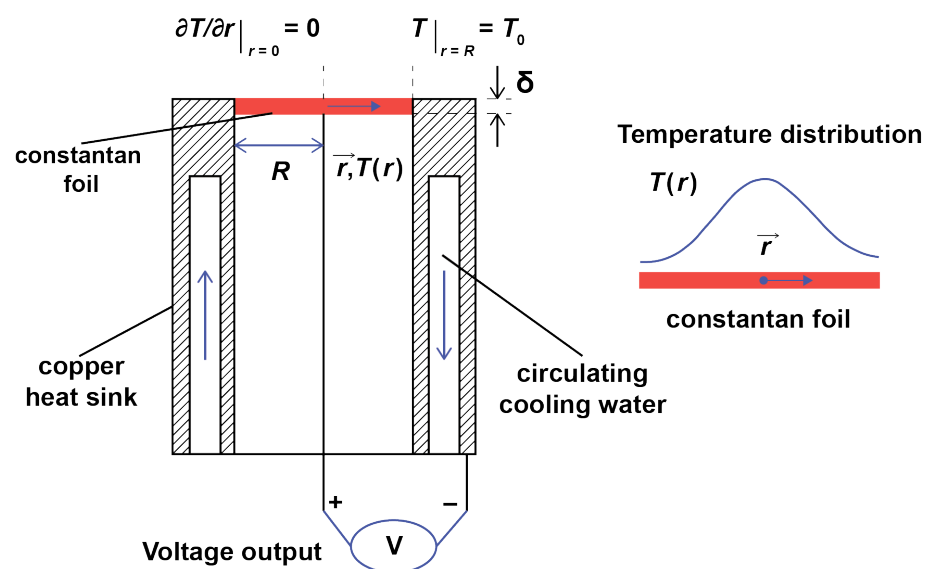

Figure 1. Sketch of Gardon heat flux gauge for convective heat transfer measurements [4].

The copper conductor is attached to the center of the foil, forming one copper-constantan (T-type) thermocouple at the junction. The second connection is formed along the edges of the constantan disk, at the point of contact with the copper radiator.

Thermal radiation moves evenly downwards at the surface of the constantan disk, which is a sensitive element. As a result, it is radially transferred to a copper radiator, which is kept cool by an internal cooling circuit by cold water. Thus, the temperature difference between the center and periphery of the disk is determined, followed by calculation of the heat flux. The Gardon Gauge has proven itself well in various fields, including measurement of heat flux in furnaces of power boilers and industrial furnaces [5], measurements of concentrated solar radiation [6], studies of heat transfer during the entry of spacecraft at hypersonic velocity into the Earth's atmosphere [4], and more.

Sensors based on hyperthermocouples [4,7–11] are widely used in the study of heat transfer processes; however, they have an unavoidable drawback. The disadvantage in this case is their thickness, which is related to both sensitivity and response time. This article discusses an experimental probe that uses a gradient heat flux sensor (GHFS), which has a radically different principle of operation.

2. Experimental Procedure

2.1. Gradient Heatmetry

Gradient heatmetry is an innovative research method based on the use of gradient heat flux sensors (GHFS). These sensors are made of materials with thermal conductivity, electrical conductivity, and thermo-EMF coefficient anisotropy. Such materials are called anisotropic thermopower elements (ATE). Due to the fact that the GHFS is made of ATE, sensor operation is based on the transverse Seebeck effect; when affected by heat flux, GHFS generates thermo-EMF $\vec{E}$ normally with respect to the heat flux per unit area vector $\vec{q}$ and proportionally to the heat flux rate (Figure 2a). Mathematically, the relationship between the heat flux and the generated thermo-EMF is expressed by

$$E_\perp = S_0 A q, \tag{2}$$

where $E_\perp$ is the thermo-EMF (mV), S_0 is the GHFS volt-watt sensitivity (mV/W), A is the GHFS plan-area (m^2), and q is the heat flux (W/m^2). The volt-watt sensitivity is determined by the thermo-EMF and conductivity tensor components, as well as by the ATE width. Furthermore, there is maximum volt-watt sensitivity which can be achieved by optimally angular deflection of the ATE trigonal plane [12].

To estimate the sensitivity, GHFSs should be calibrated in an operational temperature range determined based on the individual experiment. When calibrating, it is necessary to obtain the dependence of the volt-watt sensitivity at temperature $S_0 = S_0(T)$. GHFS are calibrated on special benches [12].

There are several methods of GHFS construction. Battery GHFS are made on the basis of 0.9999-purity single-crystal bismuth (Figure 2), which has natural anisotropic properties [13].
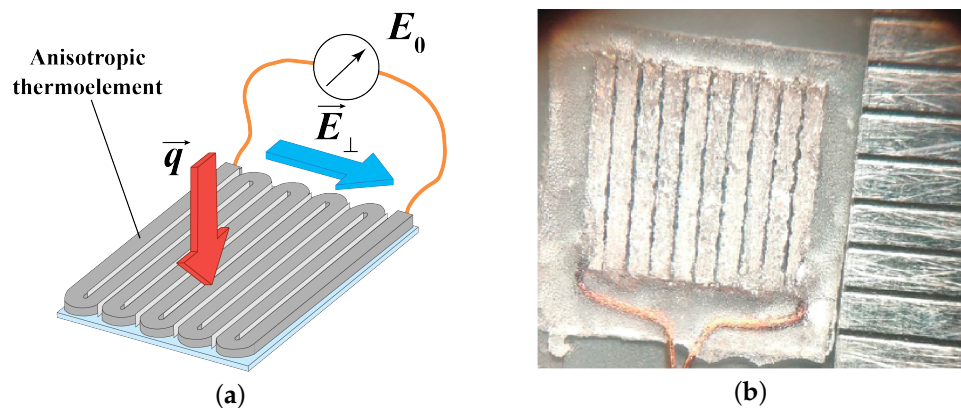

(a)   (b)

Figure 2. GHFS scheme (**a**) and general view (**b**) [14]: 1—anisotropic thermopower element (ATE); 2—mica; 3—bismuth soldering; 4—current leads; 5—lavsan base.

Despite the high (about 5...10 mV/W) volt-watt sensitivity and fast response time ($10^{-8}...10^{-9}$ s), a bismuth-based GHFS has a low temperature limit not exceeding the melting point of bismuth (544 K) [15].

In 2007, researchers at Peter the Great St. Petersburg Polytechnic University created synthetic GHFS based on layered composites of metals, alloys, and semiconductors [14]. These are referred to as heterogeneous gradient heat flux sensors (HGHFS) (Figure 3).
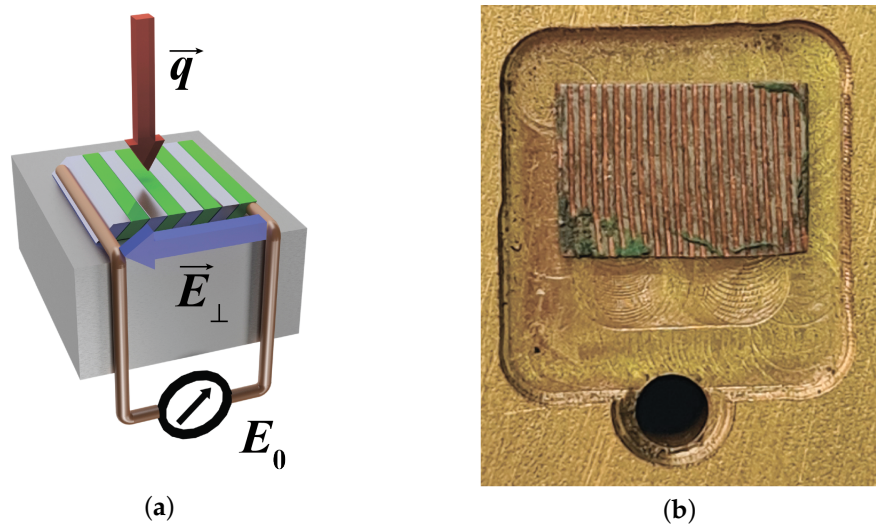
(**a**)

(**b**)

Figure 3. HGHFS scheme (**a**) and general view (**b**).

Sensors of this type demonstrate high temperature limits (up to 1300 K); essentially, the composite is a synthetic anisotropic single crystal. Therefore, the theory of GHFS is applicable to HGHFS.

GHFS and GHFS-based measuring devices have proven to be possible and reasonable for use in determining temperature, the flow rate of liquid or gas, frictional shear stress, electric current power, etc. It is worth noting that HGHFS has been proven in the study of steam condensation [16] and water boiling [17] as well.

2.2. Experimental Setup

The experimental setup used here includes a measuring probe and a frame, allowing for the possibility of use with a gas or diesel burner. A probe with HGHFS for adjustment and diagnosing the burner was created. The pipe-in-pipe probe has an HGHFS mounted on a measuring insert (Figure 4). A similar design with thermocouples has been used by other researchers [3]. In our probe, temperature measurement is combined with gradient heatmetry. The temperature measurement is then used to verify the HGHFS calibration.
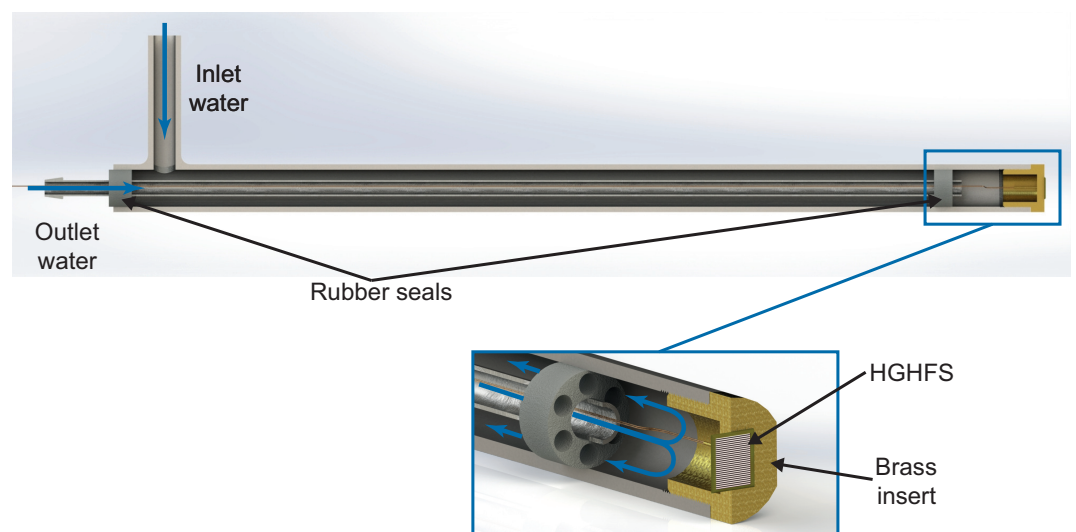

Figure 4. Experimental probe scheme.

During the design of the probe, we considered the following main factors:

1. The measuring insert dimensions must be small enough in comparison with the the flame size and large enough in comparison with the HGHFS plan-area.

2. The measuring insert must be made of a material with high thermal conductivity, and the probe itself must be made of a material with low thermal conductivity.
3. The dimensions of the probes and inserts should be convenient for mounting thermocouples and HGHFS, outputting wires, and supplying cooling water.

Here, the probe consists of a casing made from stainless steel, a coolant pipe, and a measuring insert (Figure 5) with high thermal conductivity made of brass.
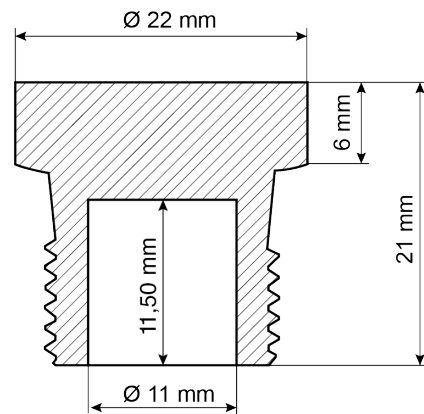
Figure 5. Measurement insert design.

The HGHFS is mounted on the end face of the brass insert. A K-type thermocouple is mounted near it. A similar thermocouple is installed on the opposite side of the insert. The probe enables measurement of the local heat flux when the power-generating equipment is operating. The data obtained by gradient heatmetry make it possible to investigate the operating mode in detail and adjust the fuel mass flow rate with high accuracy.

The multi-operation setup (Figure 6) allowed us to test burners of different power. In our experiments, we used two OILON burners [18].
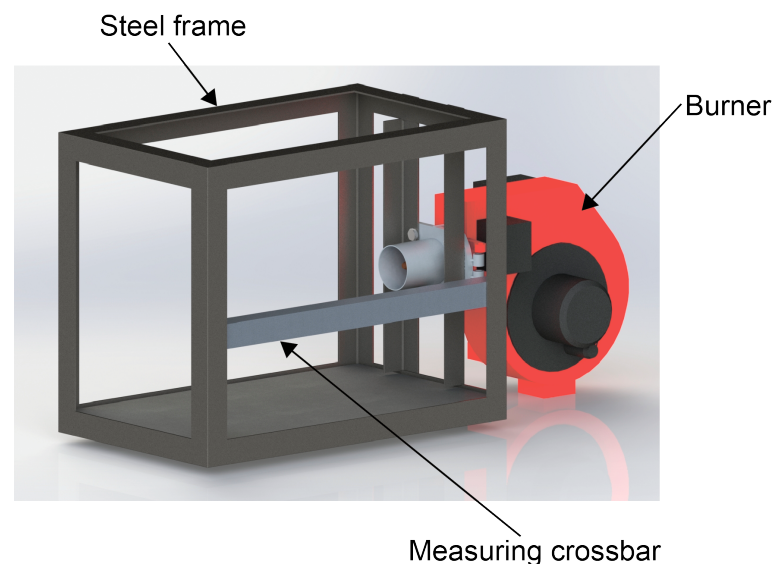
Figure 6. Experimental setup for measuring the heat flux during combustion: 1—metal frame; 2—burner; 3—crossbar with divisions.

The setup is equipped with a limiting crossbar parallel to the flame axis for probe precise positioning. The probe moves along the flame axis with a fixed pitch of 25 mm. This experiment enabled us to determine how the local heat flux from the flame is distributed along its length.

2.3. Measurement Uncertainty

Uncertainty calculations were carried out according to ISO/IEC GUIDE 98-1:2009—Uncertainty of Measurement [19], according to which uncertainty of measurement is the expression of the statistical dispersion of the values attributed to a measured quantity. The combined standard uncertainty of $y = f(x_1, x_2 \ldots x_i)$ is calculated by the following formula:

$$U_y = \pm\sqrt{\sum \left(\frac{\partial f}{\partial x_i} U_{x_i}\right)^2}, \tag{3}$$

where $\frac{\partial f}{\partial x_i} U_{x_i}$ is the dispersion of x_i. The values of U_{x_i} were assumed to be known and were determined by the characteristics of the devices.

Factors contributing to uncertainty in heat flux measurements are:

- Error in the GHFS volt-watt sensitivity
- Error in measuring the GHFS area
- Errors in measurement using ADC

These errors should be evaluated as type B uncertainties, as follows:

$$U_q = \sqrt{\left(\frac{\partial q}{\partial E} U_E\right)^2 + \left(\frac{\partial q}{\partial A} U_A\right)^2 + \left(\frac{\partial q}{\partial S_0} U_{S_0}\right)^2}. \tag{4}$$

where q is counted according to Formula (2) and the standard uncertainty of the GHFS area, that is U_A, is equal to 2.8×10^{-8} m^2. Here, the standard uncertainty of the GHFS volt-watt sensitivity, U_{S_0}, was assumed to be equal to 0.17 mV/W. In the experiments, a multimeter Fluke 287 was used to register the signal and U_E was equal to 0.025% [20];

To estimate the extended uncertainty, the coverage factor was $K = 2$.

$$U_{ext} = K U_q. \tag{5}$$

As a result, we obtained the relative uncertainty when measuring the heat flux as

$$u_{ext} = \frac{U_{ext}}{q}. \tag{6}$$

As an example, Table 1 presents the results of the uncertainty calculation.

Table 1. The uncertainty budget for heat flux measurement (diesel flame; diesel mass flow rate G3 = 7.95 kg/h; x = 125 mm).

Quantity	Value	Standart Uncertainty	Probability Distribution	Sensitivity Coefficient	Uncertainty Contribution
S_0, mV/W	4.97	0.17	B	−7238	1230.5
A, m^2	25×10^{-6}	2.8×10^{-8}	B	-144.2×10^5	40.32
E, mV	4.488	0.025	B	16.1×10^3	401.6
q, W/m^2	36.05×10^3	1295.0	B		
u_{ext}, %		7.18			

Analysing the contribution of the uncertainty showed that the greatest influence is conferred by the assessed accuracy of the volt-watt sensitivity S_0. Within the framework of the proposed method, it is possible to improve the accuracy of heat flux measurement by refining the volt-watt sensitivity and using a more accurate thermo-EMF meter.

3. Experimental Results

3.1. Pilot Experiments

Pilot experiments were carried out using a household gas burner. The scheme of the experiments is shown in Figure 7.
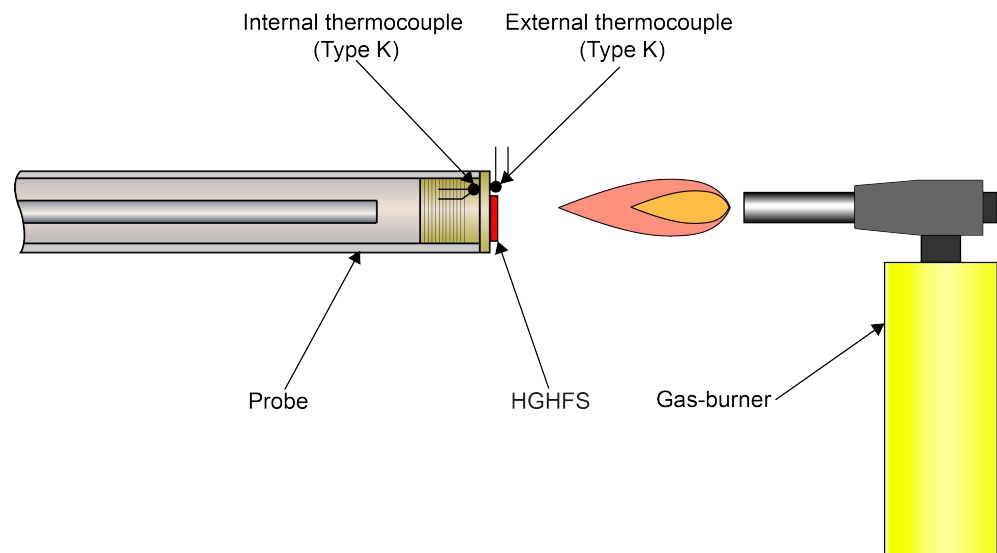

Figure 7. Pilot study scheme.

The probe was mounted horizontal and blown by the flame from the burning gas. This experiment simulates the technique for obtaining a uniform temperature field, similar to an infinite plate, which simplifies the calculation of the heat flux per unit area and makes it possible to compare the results of the HGHFS and thermocouples. The data from two thermocouples and the sensor were recorded on a National Instruments analog-to-digital converter (ADC). We compared the heat flux per unit area measured by the HGHFS q_{HGHFS} with the heat flux calculated from the heat transfer of the plate with known surface temperatures $q_{thermocouples}$ [21]:

$$q_{thermocouples} = k \frac{T_{ext} - T_{int}}{\delta}, \tag{7}$$

where $k = 110$ W/(m×K) is the thermal conductivity of the metal block, T_{ext} and T_{int} are the temperature (in K) on the external and internal surfaces of the insert, respectively, and δ is insert thickness (m).

The results of the comparison are shown in Figure 8.

Figure 8 demonstrates that the average heat fluxes measured by the HGHFS and calculated based on the thermocouple measurements are quite similar. Because the insert is 11 mm thick, the fluctuations in heat flux determined by the temperature measurement data are insignificant. HGHFS is not related to the thermal lag of the insert; therefore, we observe heat flux fluctuations. The disarrangement between time-averaged $\bar{q}_{HGHFS}$ and $\bar{q}_{thermocouples}$ does not exceed 3%.

We estimate the relative extended uncertainty of heat flux measurements about at 7%; thus, gradient heatmetry provides satisfactory results in the burning investigation.
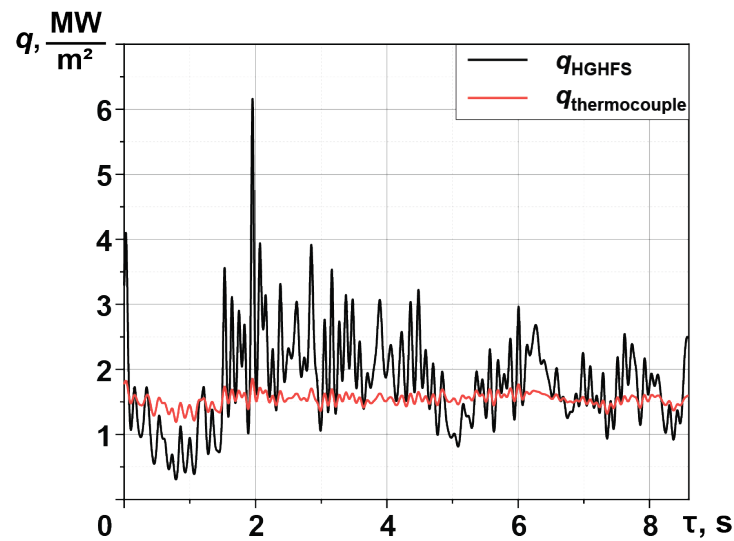
Figure 8. Heat flux graph for pilot studies.

3.2. Gas Flame

Currently, the vast majority of power plants use conventional gas as fuel. This is due to its simplicity of combustion, lack of preparatory procedures, and low level of pollutant emissions.

Here, we consider the heat generated by a gas flame produced by an OILON GP-6 burner [18]. The burner was mounted on the frame (Figure 6), which allowed us to investigate the heat generation along the length of the flame. Propane was used as fuel.

The combustion mode was selected in such a way as to obtain stable burning. In this operating mode, it was possible to burn gas quite efficiently (Figure 9). Propane burning with the optimal stoichiometric ratio is not accompanied by radiation in the visible spectrum.


Figure 9. Propane combustion in OILON burner.

The flame turns blue as fuel and oxidant exit the burner head, which is when the gas with the largest amount of oxidant is burning. The process is then stabilized, and radiation in the visible spectrum is not observed. The results of measuring the flame heat flux are shown in Figure 10.

According to our data, three combustion zones can be distinguished. In the "cold" flame zone ($x = 0. . .150$ mm from the burner nozzle), the fuel is actively mixed with the oxidant, and small part of the fuel burns. The active combustion zone ($x = 150. . .350$ mm from the nozzle) is the area in which the optimal ratio of fuel and oxidant is maintained and maximum heat generation is observed. In the "tail" zone ($x > 350$ mm), the remaining fuel burns out.

The theoretical chemical reaction of propane air oxidation has the form [1]

$$C_3H_8 + 5O_2 = 3CO_2 + 4H_2O. \tag{8}$$
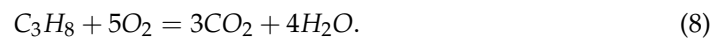
In the our experiments, the flame temperature did not reach 2000 °C; therefore, the formation of NO_x in Equation (8) can be ignored.

The heat balance equation for the reaction in (8) is

$$Q_{fl} = Q_{comb} - Q_{C_3H_8} - Q_{air} - Q_{CO_2} - Q_{H_2O}, J \tag{9}$$

where Q_{fl} is the actual heat generated during the combustion of gas, Q_{comb} is the heat generated during the combustion of propane, $Q_{C_3H_8}$ is the heat needed to heat propane by the activation temperature, Q_{air} is the heat needed to heat the air to the activation temperature, Q_{CO_2} is the heat carried away by the exhaust gases, and Q_{H_2O} is the heat carried away by water. The calculation was performed for the temperature of $t = 965$ °C measured by thermocouple during the experiment.

Substituting the mass flow rates calculated for the theoretical chemical reaction (8) provides $Q_{fl} = 36.6$ kW. Experimental and theoretical values were compared according to the heat flux. The integral heat flux obtained in the experiment was $q_{exp} = 71.7$ kW/m^2, with the theoretical calculation $q_{theor} = 73.6$ kW/m^2. This again proves the applicability and efficiency of this methodology in the study of flame combustion.

As shown above, the average heat flux obtained in the experiment and the heat flux calculated theoretically are comparable; however, the theory does not allow for the local heat flux to be calculated. Figure 10 demonstrates the high unevenness of heat generated from the flame ($q'_{max} = 98.7$ kW/m^2 , $q'_{min} = 3.1$ kW/m^2). This suggests that it is possible to determine the zone of local overheating of the heat transfer surfaces and efficiently adjust the burner. This last conclusion opens up new perspectives on boiler design. Data on the the heat flux unsteadiness in terms of both time and surface area allows these factors to be taken into account when calculating and designing heat exchange surfaces.
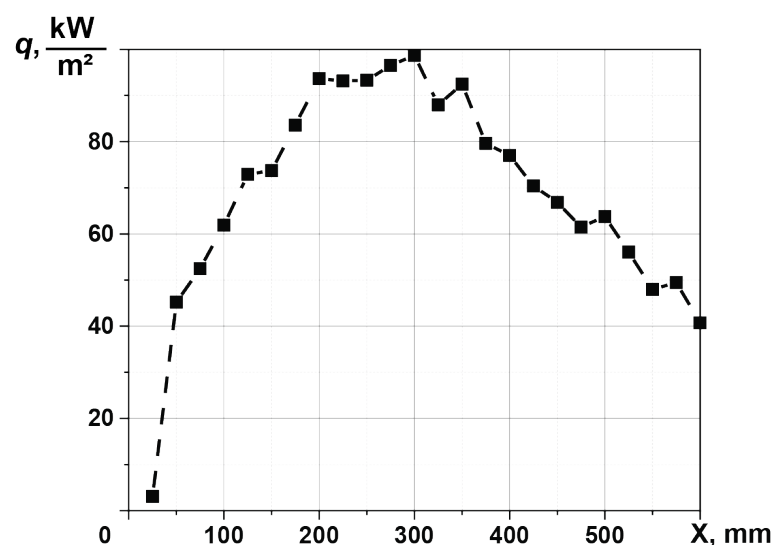

Figure 10. Local heat flux along the gas flame.

3.3. Diesel Flame

The main problem with fire-tube boilers is burnout of the fire tube caused by uneven heat generation, leading to uneven scale deposition. Burnout of the fire tube can lead to a steam explosion and failure of the entire power plant.

Here, we consider the combustion of diesel fuel in an OILON KP-6 burner with a DANFOSS nozzle, a mass flow rate of 1.75 gallons, and a flame coning angle of 60° [22]. The nozzle is an important element of the burner, and can easily become clogged and fail. It is impossible to assess its operability and compliance with factory settings when the burner is in operation.

The operating mode of the burner was selected in such a way as to obtain a steady flame (Figure 11).

Figure 11. Diesel fuel combustion in OILON burner.

Burning of diesel fuel during combustion is a complex and ambiguous chemical process, and a large number of assumptions are necessary in order to calculate it [23]. When solving this problem in relation to boiler equipment, it is sufficient to consider the local heat generation and temperature field. Figure 12 shows the values of the local heat flux for a fuel mass flow rate of 7.11 kg/h.
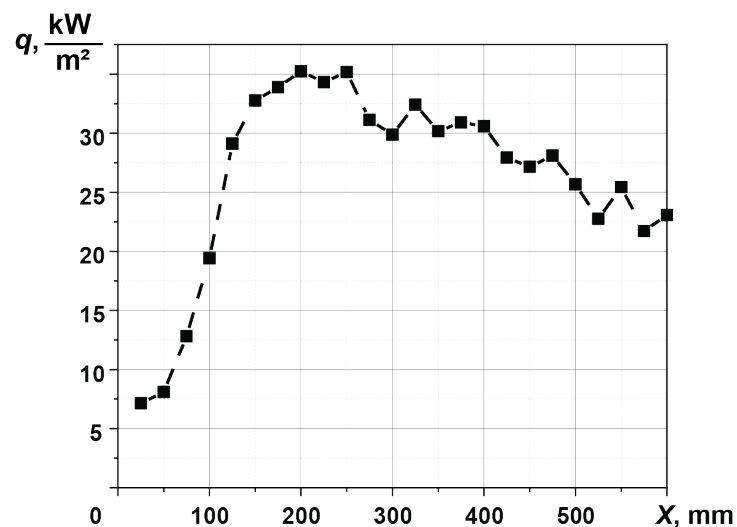

Figure 12. Local heat flux along the diesel flare.

Similar to the gas flame, three combustion zones can be distinguished: a zone of "cold" flame ($x = 0 \ldots 150$ mm from the burner nozzle), an active combustion zone ($x = 150 \ldots 300$ mm from the burner nozzle), and a "tail" zone ($x > 300$ mm) in which the flow is destabilized and the remaining fuel burns out. The tail zone features heat flux fluctuation associated with peculiarities of the flame. Because liquid fuel combustion is considered diffusive, the destabilization of the heat flux leads to the emergence of separate sources of active combustion.

Figure 13 shows the temperature field measured in the central section of the flame. Measurements were conducted by the contact method using a K-type thermocouple. The elapsed time of the K-type thermocouple at temperatures above 1000 was experimentally determined. In our experiments, the temperature measurement time at each point was about 100 s, meaning that our results can be considered correct.

Temperature fluctuations were observed at a distance of 300 mm from the outlet section of the "burner head", similar to the heat flux per unit area measured by the HGHFS.

The burning of a drop of liquid fuel in an oxidant is modeled as a stationary sphere, from the surface of which the fuel evaporates and reacts with the oxidant. It is impossible to calculate the flame heat generation in such a setting. When the flow is swirled, drops combine and leave the combustion area due to inertia or gravity. It is almost impossible to take this into account during calculations, and as a result it is impossible to calculate the thermal balance. If we consider a certain number of drops close to one another, we have a surface that is in direct contact with the oxidant, which results in combustion.
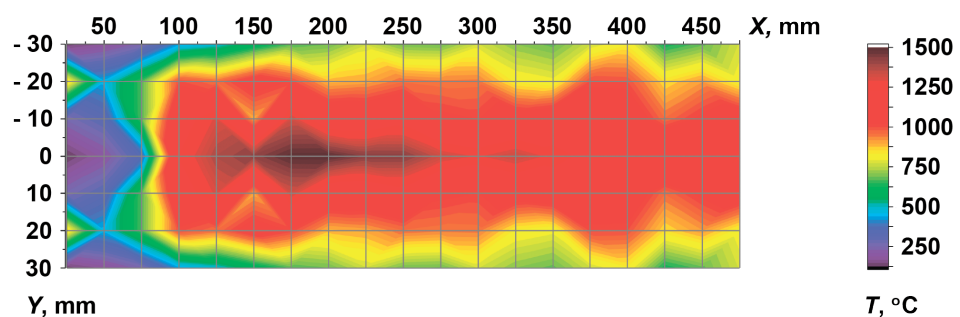

Figure 13. Temperature field in the cross-section of the diesel flame.

Here, let us make such an assumption and consider the heat transfer radiated from the flame as one from a solid body with a temperature equal to the temperature at the periphery of the flame. The flame emissivity of a liquid-fuel flame is close to 1.0; therefore, the heat flux from the flame according to the Stefan–Boltzmann law is [1]

$$q_{calc} = c_0 \varepsilon \left[\left(\frac{\overline{T}_{fl}}{100} \right)^4 - \left(\frac{T_{probe}}{100} \right)^4 \right], \tag{10}$$

where q_{calc} (W/m^2) is the calculated flame heat flux, $\overline{T}_{fl}$ (K) is average temperature of the flame periphery, and T_{probe} is the temperature on the surface of the probe (313 K). The calculation according to the Formula (10) provides $q_{calc} = 31.6$ kW/m^2, and the average integral heat flux obtained in the experiment is $q_{exp} = 28.6$ kW/m^2. The discrepancy of 9.5% in such an experiment can be considered acceptable.

The OILON KP-6 burner is designed for a wide range of diesel mass flow rates; here, we have only considered modes with a stable flame (6.49...8.58 kg/h). The local heat flux distributions are shown in Figure 14. The curves show that the "cold" flame zone is independent of the mass flow rate. The main difference between the operating modes is the distance from the nozzle, where the local heat flux is at a maximum, as well as the fluctuation magnitude in the flame tail zone. The operating mode corresponding to the mass flow rate of 7.95 kg/h is the most stable and active.
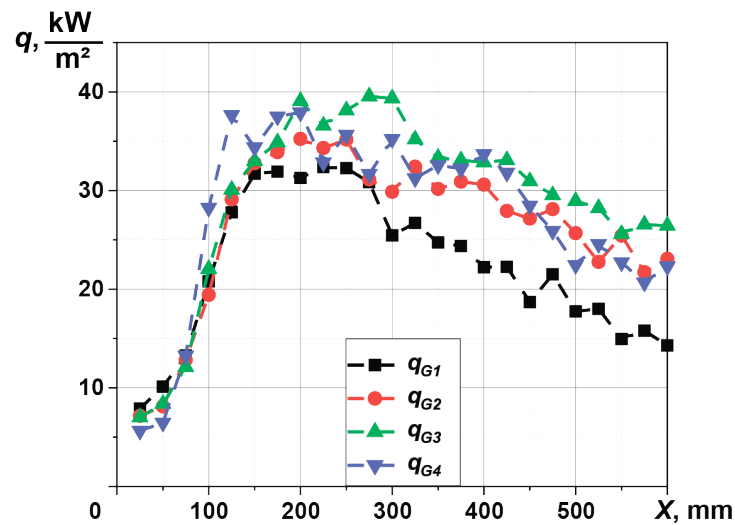
Figure 14. Dependence of the local heat flux on the longitudinal coordinate at various fuel mass flow rates: q_{G1} = 6.5 kg/h, q_{G2} = 7.1 kg/h, q_{G3} = 7.95 kg/h, q_{G4} = 8.6 kg/h.

Due to the peculiarities of the experimental setup it, is incorrect to talk about measuring the absolute pollutant emissions in the exhaust gases. It is impossible to track the air inflow from the atmosphere or the focusing of the exhaust gas flow for accurate measurement. Data on the exhaust gases are presented in relative values as relates to the maximum values. To assess the effect of fuel consumption on toxic emissions, the Testo 330i gas analyzer was used [24]. The results of the analysis are presented in Table 2.

Table 2. Relative pollutant emission concetration $\widetilde{C}_i$ depending on the diesel mass flow rate.

Flow-Rate, kg/h	CO_2	nCO	O_2
7.11	0.80	1.00	0.92
7.95	0.62	0.22	1.00
8.58	1.00	0.07	0.84

The relative concentration of pollutant emission depending on the mass flow rate is calculated by the formula

$$\widetilde{C}_i = \frac{C_i}{C_{max}}, \tag{11}$$

where $\widetilde{C}_i$ is the relative concentration of a substance at a specified fuel mass flow rate, C_i is the concentration of a substance at a specified fuel mass flow rate, and C_{max} is the maximum concentration of a substance.

Unfortunately, the Testo 330i gas analyzer does not allow evaluation of NO_x. In the future, we plan to use a gas analyzer that allows for measuring these parameters with high accuracy, then to analyze them in detail.

The optimal operation determined by the gradient heatmetry does not exceed the level of emissions compared to lower and higher consumption.

4. Conclusions

Despite the wide variety of probes and inserts used to determine the heat flux per unit area in the furnaces of boiler equipment, these probes are currently all based on the temperature measurement method. This approach has a number of disadvantages that mean it cannot be considered the only correct way to measure the heat flux.

Here, we have developed a unique cooled probe with HGHFS installed. The implementation of the transverse Seebeck effect with the HGHFS avoids the disadvantages described above. Therefore, it can be assumed that the gradient heatmetry is more reliable for determining the heat flux per unit area from the burner flame.

A pilot experiment in which the heat flux was compared using both temperature measurements (as most authors do) and gradient heatmetry showed the adequacy and applicability of the proposed method. At the same time, unlike thermocouples, HGHFS has a fast response time, making it possible to measure the slightest fluctuations during operation of the burners.

Comparison of the experimental values of the heat flux from the flame with the calculated values showed the reliability of our results. The discrepancy between the experimental and calculated values did not exceed 10%.

Based on the obtained temperature fields and distribution of the heat flux per unit area, it was possible to determine three main combustion zones realized during flaring of any fuel. Based on the gradient heatmetry data and gas analysis of the concentration of flue gases, it was possible to select and justify the choice of the most efficient mode of operation of the OILON KP-6 diesel burner.

This approach allows a reliable method for controlling heat generation in the furnace of any boiler equipment to be organized, permitting greater fine-tuning of industrial burners and the determination of their optimal operating mode.

Abbreviations

The following abbreviations are used in this manuscript:

LHV	Lower Heating Value
GHFS	Gradient Heat Flux Sensor
ATE	Anisotropic Thermoelemnt
HGHFS	Heterogeneous Gradient Heat Flux Sensor
ADC	Analog to Digital Converter

References

1. Glassman, I.; Yetter, R.A.; Glumac, N.G. *Combustion*, 5th ed.; Elsevier: Amsterdam, The Netherlands, 2014; 757p.
2. Kemelman, D.N.; Eskin, N.B.; Davidov, A.A. *Adjustment of Boiler Installations: Handbook*, Energiya Publ.: Moscow, Russia, 1976; p. 344.
3. Zhang, D.; Shi, H.; Meng, C.; Wu, Y.; Zhang, H.; Zhou, W.; Ran, S. Measurements on Heat Flux Distribution in a Supercritical Arch-Fired Boiler. In *Clean Coal Technology and Sustainable Development*; Yue, G., Li, S., Eds.; Springer: Singapore, 2016; pp. 207–212.
4. Martucci, A.; De Gregorio, F.; Musto, M.; Petrella, O.; Marciano, L.; Rotondo, G.; Gaudino, E. Innovative calibration methodology for gardon gauge heat flux meter. In Proceedings of the IEEE 7th International Workshop on Metrology for AeroSpace (MetroAeroSpace), Pisa, Italy, 22–24 June 2020; pp. 288–293.
5. Pullins, C.A.; Diller, T.E. Direct Measurement of Hot-Wall Heat Flux. *J. Thermophys. Heat Transf.* **2012** *26*, 430–438.
6. Guillot, E.; Alxneit, I.; Ballestrin, J.; Sans, J.L.; Willsh, C. Comparison of 3 heat flux gauges and a water calorimeter for concentrated solar irradiance measurement. *Energy Procedia* **2014**, *49*, 2090–2099.
7. Northover, E.W.; Hitchcock, J.A. A heat flux meter for use in boiler furnaces. *J. Sci. Instrum.* **1967**, *44*, 371–374.
8. Arai, N.; Matsunami, A.; Churchill, S.W. A review of Measurements of Heat Flux Density Applicable to the Field of Combustion Experimental. *Therm. Fluid Sci.* **1996**, *12*, 452–460.
9. Schulte, E.H.; Kohl, R.F. A review of measurements of heat flux density applicable to the field of combustion. *Exp. Therm. Fluid Sci.* **1969**, *40*, 1420–1427.
10. Hager, N.E., Jr. Thin Foil Heat Meter. *Rev. Sci. Instrum.* **1965**, *36*, 1564–1570.
11. Klems, J.H.; DiBartolomeo, D. Large-area, high-sensitivity heat-flow sensor. *Rev. Sci. Instrum.* **1982**, *53*, 1609–1612.
12. Mityakov, A.V.; Mityakov, V.Y.; Sapozhnikov, S.Z.; Chumakov, Y.S. Measurement of Instantaneous Values of a Heat Flux on a Vertical Heated Surface under Conditions of Free-Convection Heat Transfer. *High Temp.* **2002**, *40*, 620–625.

13. Sapozhnikov, S.Z.; Mityakov, V.Y.; Mityakov, A.V. Bismuth-Based Gradient Heat-Flux Sensors in Thermal Experiment.*High Temp.* **2004**, *42*, 629–638.
14. Sapozhnikov, S.; Mityakov, V.; Mityakov, A. *Heatmetry: The Science and Practice of Heat Flux Measurement*; Springer International Publishing: Berlin/Heidelberg, Germany, 2020.
15. Sapozhnikov, S.Z.; Mityakov, V.Y.; Seroshtanov, V.V.; Gusakov, A.A. The Combination of PIV and Heat Flux Measurement in Study of Flow and Heat Transfer Near a Circular Finned Cylinder. In Proceedings of the International Conference on Optical Methods of Flow Investigation, Moscow, Russia, 24–28 June 2019; Volume 1412.
16. Mityakov, V.Y.; Sapozhnikov, S.Z.; Zainullina, E.R.; Babich, A.Y.; Milto, O.A.; Kalmykov, K.S. Gradient Heat Flux Measurement while Researching of Saturated Water Steam Condensation. In Proceedings of the International Conference "Problems of Thermal Physics and Power Engineering" (PTPPE-2017), Moscow, Russia, 9–11 October 2017; Volume 891.
17. Sapoznikov, S.Z.; Mityakov, V.Y.; Gusakov, A.A.; Pavlov, A.V.; Bobylev, P.G. Gradient Heatmetry for Boiling of Underheated Water on Spherical Surface. *J. Phys. Conf. Ser.* **2020**, *1683*, 1683.
18. Available online: https://oilon.spb.ru/ (accessed on 11 November 2022).
19. ISO/IEC Guide 98-1:2009–Uncertainty of Measurement—Part 1: Introduction to the Expression of Uncertainty in Measurement. Available online: www.iso.org/standard/ (accessed on 12 November 2022).
20. Available online: https://flukeshop.ru/multimetr-fluke-287/ (accessed on 30 November 2022)
21. Benjamin, G. *Heat Transfer*; McGraw-Hill: New York, NY, USA, 1961; p. 454.
22. Available online: https://www.danfoss.com/ (accessed on 11 November 2022).
23. Lakshminarayanan, P.A.; Aghav, Y.V. *Modelling Diesel Combustion*; Springer: Berlin/Heidelberg, Germany, 2010.
24. Available online: https://www.testo.ru/ (accessed on 13 November 2022)